Single-Cell Analysis

International Edition: DOI: 10.1002/anie.201606039
German Edition: DOI: 10.1002/ange.201606039

Detection of Isoforms Differing by a Single Charge Unit in Individual Cells

*Augusto M. Tentori[+], Kevin A. Yamauchi[+], and Amy E. Herr**

Abstract: *To measure protein isoforms in individual mammalian cells, we report single-cell resolution isoelectric focusing (scIEF) and high-selectivity immunoprobing. Microfluidic design and photoactivatable materials establish the tunable pH gradients required by IEF and precisely control the transport and handling of each 17-pL cell lysate during analysis. The scIEF assay resolves protein isoforms with resolution down to a single-charge unit, including both endogenous cytoplasmic and nuclear proteins from individual mammalian cells.*

Questions linger regarding how genome and transcriptome variations manifest as functional proteomes, especially among populations of individual cells.[1–2] Functional proteomes are dictated by dynamic protein expression, as well as chemical modifications and splice variants of the expressed proteins. These chemical modifications yield protein variants (proteoforms) with unique functions.[3] Nucleic acid measurements (for example, RNA-seq) fundamentally cannot measure specific proteoforms (that is, post-translational modifications and alternative splicing). However, direct measurement of proteins in single cells, predominantly by immunoassays,[4–6] is limited by both the availability and selectivity of immunoreagents (for example, antibodies).[7] Challenges in the generation of proteoform-specific antibodies limit our understanding of the roles proteoforms play. Surmounting this cytometry bottleneck requires the introduction of new tools optimized for proteoform analysis.[8]

Mass spectrometry is currently the workhorse technology for proteomic analysis. Bottom-up mass spectrometry digests proteins into peptides and identifies proteins and post-translational modifications from the mass spectra of the peptides.[9] However, owing to the digestion of proteins into peptides, it is challenging to determine how the modified peptides relate back to the intact proteins (for example, one proteoform with many modifications or multiple proteoforms with fewer modifications).[10] Top-down mass spectrometry can identify and measure specific proteoforms by using separations to reduce the sample complexity and avoid digestion of the proteins of interest.[11] While mass spectrometry is able to identify and quantify specific proteoforms, the analytical sensitivity is insufficient for single-cell proteoform cytometry.[11,12]

As a complimentary approach to mass spectrometry, microfluidic separations facilitate the selective profiling of proteoforms in single cells. In recent work, polyacrylamide gel electrophoresis (PAGE) was combined with a subsequent immunoassay for single-cell western blotting.[13] Although western blotting is a high-selectivity protein assay, post-translational modifications and alternative splicing do not always yield resolvable molecular mass differences. Fortunately, even proteoforms of similar mass often exhibit isoelectric point (pI) differences that are readily detectable with another electrophoretic assay, namely, isoelectric focusing (IEF).[14] Capillary IEF followed by immunoblotting has resolved protein post-translational modifications in lysates pooled from as few as 25 cells.[15]

To separate proteins by pI, IEF employs protein electromigration along a stable pH gradient.[16] Proteins electromigrate until each species enters a region of the pH gradient in which the local pH is equal to the pI of that species; at that location, the proteoform has no net mobility. Electromigration therefore halts and the protein is focused. IEF has immense resolving power and selectivity; even single-charge differences among proteoforms are detectable.[17]

To extend the power of IEF from pooled lysates to individual cells, we designed a 3D microfluidic device that integrates all preparatory and analytical stages for single-cell IEF with in-gel immunoprobing (cell isolation, lysis, IEF, UV-actuated blotting, and probing). Microfluidic integration is essential to overcoming diffusion-based dilution of the lysate from a single cell. This dilution is a loss mechanism that is exacerbated by sample handling in multi-stage assays, including immunoblotting. Although proteins can have appreciable intracellular concentrations (ca. 20 nM in a 30 μm diameter cell),[18,19] a diffusion time of 5 s can reduce the maximum protein concentration by 90% (see Supporting Information). Microfluidic integration minimizes the time allowed for diffusion-driven dilution, thus making isoform detection by electrophoretic analysis of single-cell lysates possible.

To control scIEF, we designed a multilayered polyacrylamide gel device capable of integrating all required chemistries without pumps or valves (Figure 1a). The device comprises a glass slide coated with a bottom gel layer for isolating single cells in microwells by gravity sedimentation

[*] A. M. Tentori,[+] K. A. Yamauchi,[+] Prof. Dr. A. E. Herr
The UC Berkeley/UCSF Graduate Program in Bioengineering
Berkeley, CA (USA)
A. M. Tentori[+]
Department of Chemical Engineering
Massachusetts Institute of Technology
Cambridge, MA (USA)
Prof. Dr. A. E. Herr
Department of Bioengineering, UC Berkeley
308B Stanley Hall, Berkeley, CA 94720 (USA)
E-mail: aeh@berkeley.edu
[+] These authors contributed equally to this work.
Supporting information and the ORCID identification number(s) for the author(s) of this article can be found under: http://dx.doi.org/10.1002/anie.201606039.

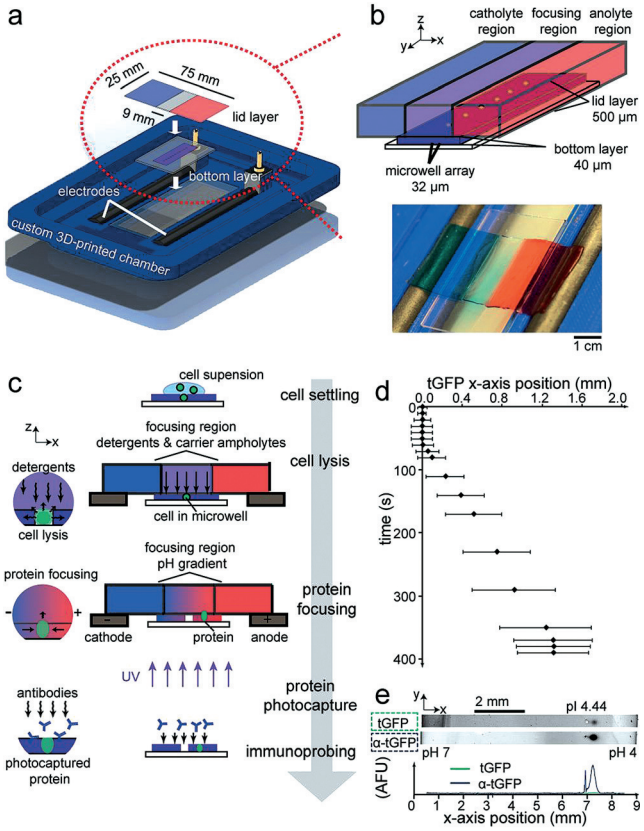

Figure 1. Direct measurement of proteins using scIEF. a) Exploded view of the scIEF assay setup. b) Isometric schematic of the multilayer scIEF microdevice and top-view photograph of the lid layer with catholyte and anolyte regions with blue and red dye, respectively. c) scIEF workflow. d) Time-course of tGFP fluorescence signal position during single-cell lysis and scIEF. Error bars indicate band width (4σ). pH range, 4–9; microwell position, 4.5 mm from catholyte-side edge of the bottom gel. e) Inverted grayscale fluorescence micrographs report blotting and subsequent immunoprobing (α-tGFP) from a single cell. pH range, 4–7; microwell position, 6.75 mm from catholyte-side edge of the bottom gel. Traces are in arbitrary fluorescence units (AFU).

and a lid gel layer patterned with chemistries to control cell lysis and (after the electric field application) the formation of pH gradients for scIEF (Figure 1b). The chemically patterned lid layer consists of three different regions, with 1) a central focusing region containing both the non-ionic detergent cell-lysis buffer and the mobile buffer species (carrier ampholytes) that form the pH gradient and 2) two flanking anolyte and catholyte regions created by copolymerizing weak acrylamido acids and bases in different stoichiometries into the polyacrylamide gel (that is, Immobilines; Supporting Information, Figure S1 and Table S1).[20]

Fluidic contact between the 500-µm thick lid layer and the 10-fold thinner bottom layer diffusively imprints the chemical environment of the lid layer onto the bottom layer (Figure 1c). The free-standing lid layer is compliant (Figure 1b) and, as both the bottom layer and lid layer are fully hydrated when mated, a wetted layer at the interface ensures fluidic and electrical contact. Upon this first contact, cell lysis in each microwell is initiated by the diffusion-driven release of the mobile non-ionic lysis reagents from the lid layer into the bottom layer. To minimize evaporation during the assay, an additional glass slide is placed on top of the lid layer. At this stage, no electric potential is applied. We monitored human glioblastoma cells expressing TurboGFP (U373-tGFP) and observed the initial release of tGFP within 10 s of lid application, with the fluorescence signal filling the 32 pL microwell volume within 20 s (Figure 1d and Supporting Information, Figure S2). Electrodes mated to the flanking anolyte and catholyte regions initiate and sustain IEF, with the fluorescent tGFP peaks from each cell (signal-to-noise ratio (SNR) > 8) reaching a focused position approximately 310 s later (Figure 1d and Supporting Information, Figure S2). We characterized the repeatability of the lid placement relative to the microwells and determined the coefficient of variance (CV) of the lid position to be about 15% (Supporting Information, Figure S3). Nevertheless, precise positioning of the lid will not affect the relative positions of the focused bands because the proteins will migrate to their pI regardless of the starting position of the microwell relative to the anolyte and catholyte boundaries.

Two additional design considerations constrain diffusive losses, making the long duration (relative to fast-acting diffusion) separation possible. First, diffusive losses are limited to two spatial dimensions owing to the IEF occurring along the *x*-axis (Supporting Information, Figure S4). Second, diffusive losses in the out-of-plane dimension are notably reduced by the presence of the dense hydrogel lid layer. During both lysis and focusing, simulations show that analyte diffusivity is considerably lower into the dense gel lid, compared to that into the free solution (Figure 2a and Supporting Information, Figure S4). Empirical results corroborate the reduced out-of-plane diffusive losses as approximately 15% of the total protein signal after a remarkable 600 s of voltage application time (Figure 2b and Supporting

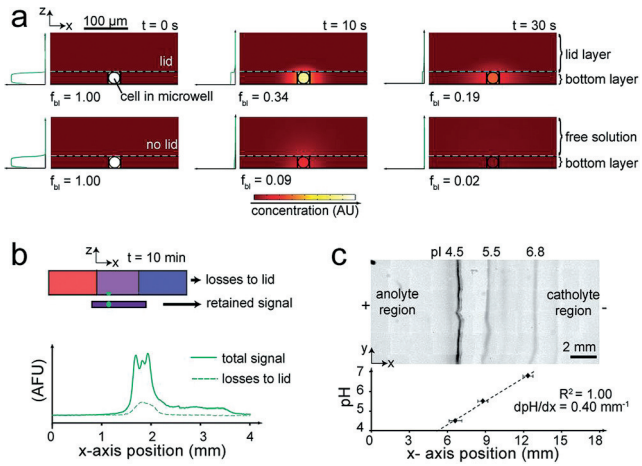

Figure 2. Control of diffusive and electrokinetic transport to establish robust, non-uniform chemistries for scIEF. a) Concentration heat maps from a simulation show that protein diffusion out of the bottom layer is mitigated in hindered (with lid) versus unhindered (no lid, free solution) conditions. Plots indicate the maximum concentration along the *z*-axis; f_{bl} = fraction of the total protein in the bottom layer. b) Fluorescence traces show tGFP transfer from the bottom layer to lid layer after 10 min of scIEF. c) Inverted grayscale fluorescence micrograph shows focused pH markers in a pH 4–7 gradient. Dashed line is a linear fit; error bars are the peak widths (4σ).

Information, Figure S5). Note that the position of the microwells in the bottom layer can be optimized to reduce diffusive losses of specific proteins by reducing the electromigration time of a protein from the microwell to its pI.

To detect endogenous isoforms, we designed a hydrogel device to support blotting of the scIEF separation and subsequent diffusive in-gel immunoprobing (Figure 1e and Supporting Information, Figure S6). By performing an immunoassay after a separation, a single antibody probe (for example, a pan-specific antibody) can detect and discern multiple, spatially separated isoforms. Our design uses a photo-active monomer (benzophenone methacrylamide) cross-linked into the bottom layer to covalently immobilize protein peaks after brief UV exposure.[13,21] The characteristic timescale of the immobilization reaction is 5.5 s.[22] Photocapture was performed with the applied electric field set to electrically floating conditions, as peak drift during photocapture confounds the pI location and reduces separation resolution (R_s).[22] We estimate that diffusion-induced peak defocusing during the 5.5 s of the immobilization reaction does not affect the pI location and reduces R_s by approximately 20%, as is consistent with our previous studies (see Supporting Information).[22] A longer (45 s) UV exposure period was used to maximize the immobilization efficiency. We experimentally measured the capture efficiency of the proteins in our system to be $17.7 \pm 1.5\%$ (Supporting Information, Figure S7), which leads to an estimated lower limit of detection of circa 42000 molecules needed in the bottom layer before photocapture for detection by immunoprobing (see Supporting Information). Immunoprobing using primary and fluorescently labeled secondary antibodies reported a major tGFP band with an SNR of 51.87 ± 39.10 ($n = 9$, Figure 1e and Supporting Information, Figure S6a). Importantly, covalent immobilization of the resolved proteins to the gel decouples time-dependent dilution considerations from all subsequent assay stages, archival storage, and multiple reprobing rounds.[13]

We next optimized scIEF resolving power to enhance the selectivity of isoform detection (Figure 2c). Adjusting the design of the chemically patterned lid layer imprints pH gradients of different length and steepness on the bottom layer, which determines the focusing time and R_s. Fluorescence flow cytometry and mass cytometry can measure up to approximately 12 and approximately 34 targets in a single cell, respectively,[23] but both techniques are unable to distinguish isoforms that lack highly selective antibodies. In contrast, in-gel immunoprobing assays with separations multiplex the product of the number of resolvable proteins (peak capacity,[24] ca. 17 for scIEF, see Supporting Information) with circa 4 spectrally distinct fluorescent dyes (labeled secondary antibodies) and 2–20 stripping/re-probing cycles (depending on the physicochemical properties of the target).[13,21,25,26]

We investigated the capability of scIEF to concurrently measure endogenous cytoskeletal and nuclear targets (for proteins with known isoforms). We assayed tGFP ($pI \approx 4.5$), β-tubulin (β-TUB, $pI \approx 5.5$), and lamin A/C in individual glioblastoma cells (Figure 3). We used secondary antibodies, each labeled with a different fluorophore (AlexaFluor 555 and 647), to discriminate between the signal from mouse (lamin A/C) and rabbit (tGFP and β-TUB) primary antibodies, demonstrating the utility of spectral multiplexing. Using a four-color laser scanner, multiplexing can be further increased using commercially available dyes (for example, AlexaFluor). Both native and denaturing scIEF were studied, as the isoform state is sensitive to sample preparation conditions. Under native scIEF, tGFP and β-TUB were well-resolved with R_s of 1.91 ± 0.36 ($n_N = 9$ cells), yielded a conservative peak capacity of 9.0 ± 3.1 (based on the width of widest peak, β-TUB), and reported no isoforms. Expression of tGFP and β-TUB were not well-correlated (Pearson correlation, $\rho = 0.22$, $p = 0.60$, Figure 3a and Supporting Information, Figure S6b).

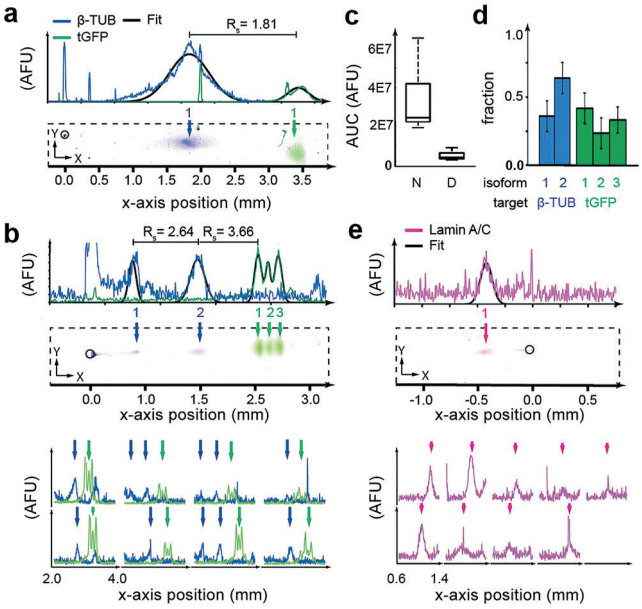

Figure 3. scIEF with immunoprobing resolves proteoforms in individual mammalian cells. a) False-color fluorescence micrographs and traces show scIEF detection by immunoprobing of β-TUB and tGFP from individual cells. Microwells are outlined with a black circle, located at 0 mm. Arrows indicate protein peaks; plotted black outlines are the Gaussian fits for identified peaks. b) False-color fluorescence micrographs and traces show detection of denatured β-TUB isoforms in 3 of 8 cells. c) Median total tGFP probing fluorescence (area under the curve, AUC) under native (N) and denaturing (D) conditions ($n_D = 8$, $n_N = 9$, $p < 0.01$). (d) Relative isoform fractions ($n_{\beta\text{-TUB}} = 3$, $n_{tGFP} = 8$). e) False-color fluorescence micrographs and traces show detection of lamin A/C from individual cells under denaturing conditions ($n_D = 9$). pH range, 4–7; microwell position, 6.75 mm from the catholyte-side edge of the bottom gel in all separations.

Under denaturing scIEF (7 M urea and 2 M thiourea added to the lysis buffer), three tGFP isoforms ($R_S > 0.88$) and two β-TUB isoforms ($R_S = 2.54 \pm 0.46$, $n_D = 3$) were detected (Figure 3b and Supporting Information, Figure S6c). The tGFP isoforms arise from differential C-terminal cleavage by non-specific proteases[17] and differ by just a single charge unit. Interestingly, the native conditions yielded 86% higher total tGFP probing signal than the denaturing conditions, which is attributed to the sensitivity of the photocapture efficiency to the protein state or, possibly, to incomplete electromigration out of the microwell, as is under study

(Figure 3c). Denaturing conditions resulted in well-resolved major β-TUB and tGFP peaks ($R_S = 1.77 \pm 0.59$) and a circa 3-fold higher peak capacity than native conditions (28.08 ± 6.68, $n_D = 8$, Figure 3d). Using the pI of the tGFP isoforms (Supporting Information, Figure S8), we estimated the pI of the β-TUB isoforms to be 5.11 and 5.76. The acidic isoform of β-TUB had a total expression approximately 5-fold higher than that of the basic isoform ($p < 0.01$, Figure 3d). β-TUB isoforms have been implicated in resistance to tubulin-binding cancer therapeutics (namely, Taxol).[27]

To assess the relevance to nuclear proteins, which are difficult to assay using classical single-cell cytometry-based techniques without fractionation,[28] we assayed U373-tGFP cells for lamin A/C (Figure 3e and Supporting Information, Figure S6d). As expected, we detected lamin A/C in all glioblastoma cells. Because of its basic pI of 6.8–7.3,[29] the lamin A/C bands migrated toward the cathode side and focused to the left of the microwell. The fluorescent readout signals observed for this set of validation proteins were sufficient (SNR > 3) for the study of endogenous isoforms from single mammalian cells. The successful immunoprobing of lamin A/C (nuclear protein), tGFP (cytosolic protein), and β-TUB (cytoskeletal protein) demonstrates that the denaturing scIEF lysis buffer solubilizes proteins from the major cellular compartments. Future work will characterize and optimize the lysis buffers for more stringent applications such as histones and other high-affinity complexes.

The number of parallel scIEF separations that can be carried out on the same chip is dictated by the microwell spacing (Supporting Information, Figure S2) and device size (which together determine the number of microwells), as well as by the cell-settling efficiency of passive sedimentation. In this work, approximately 10 cells were analyzed per chip. The number of cells analyzed per device can be increased by fabricating larger devices or using active settling methods.[30] Future work will aim to increase the throughput of the scIEF device for more robust detection of rare events. Owing to the rapid separations, the overall throughput of the assay can be increased by running multiple separations in series and then immunoprobing several devices in parallel.

Direct detection of proteoforms in single cells is a crucial capability, as protein copy numbers (especially isoforms) from single mammalian cells are only sparsely reported and RNA copy number may not always correlate well with protein expression (or form).[31] The demonstrated capability of the scIEF assay to resolve isoforms of endogenous proteins from single cells provides a much-needed capability to elucidate the role of specific proteoforms in cancer progression, cardiovascular disease, and neurodegenerative disorders.[1,32] The scIEF assay opens a separations-based avenue for measuring proteoforms, an important aspect of protein signaling that is difficult to observe with conventional cytometry tools.

Acknowledgements

The authors acknowledge members and alumni of the Herr lab for helpful discussions. Partial infrastructure support was provided by the QB3 Biomolecular Nanofabrication Center. This research was performed under a UC Cancer Research Coordinating Committee Predoctoral Fellowship (A.M.T.), a University of California, Berkeley Siebel Scholarship (A.M.T.), a National Science Foundation Graduate Research Fellowship (K.A.Y), a National Science Foundation CAREER award (CBET-1056035 to A.E.H.) and a National Institutes of Health R01 (1R01CA203018 to A.E.H.). A.M.T. and K.A.Y. performed the experiments, simulations, and data analysis. A.M.T., K.A.Y., and A.E.H conceived and designed the scIEF assay, designed the experiments, and wrote the manuscript. The authors declare financial interests. A.M.T., K.A.Y., and A.E.H. are co-inventors on patents related to single-cell analysis, and A.E.H. has a financial interest in a company that commercializes a single-cell analysis tool.

Keywords: immunoassays · isoelectric focusing · lab-on-a-chip · proteomics · single-cell analysis

How to cite: *Angew. Chem. Int. Ed.* **2016**, *55*, 12431–12435
Angew. Chem. **2016**, *128*, 12619–12623

[1] J. A. Alfaro, A. Sinha, T. Kislinger, P. C. Boutros, *Nat. Methods* **2014**, *11*, 1107–1113.
[2] S. Myhre, O.-C. Lingjærde, B. T. Hennessy, M. R. Aure, M. S. Carey, J. Alsner, T. Tramm, J. Overgaard, G. B. Mills, A.-L. Børresen-Dale, T. Sørlie, *Mol. Oncol.* **2013**, *7*, 704–718.
[3] L. M. Smith, N. L. Kelleher, *Nat. Methods* **2013**, *10*, 186–187.
[4] E. R. Zunder, E. Lujan, Y. Goltsev, M. Wernig, G. P. Nolan, *Cell Stem Cell* **2015**, *16*, 323–337.
[5] S. C. Bendall, G. P. Nolan, M. Roederer, P. K. Chattopadhyay, *Trends Immunol.* **2012**, *33*, 323–332.
[6] W. Wei, Y. S. Shin, C. Ma, J. Wang, M. Elitas, R. Fan, J. R. Heath, *Genome Med.* **2013**, *5*, 75.
[7] C. Stadler, E. Rexhepaj, V. R. Singan, R. F. Murphy, R. Pepperkok, M. Uhlén, J. C. Simpson, E. Lundberg, *Nat. Methods* **2013**, *10*, 315–323.
[8] T. Hattori, J. M. Taft, K. M. Swist, H. Luo, H. Witt, M. Slattery, A. Koide, A. J. Ruthenburg, K. Krajewski, B. D. Strahl, K. P. White, P. J. Farnham, Y. Zhao, S. Koide, *Nat. Methods* **2013**, *10*, 992–995.
[9] A. Pandey, M. Mann, *Nature* **2000**, *405*, 837–846.
[10] N. L. Kelleher, P. M. Thomas, I. Ntai, P. D. Compton, R. D. LeDuc, *Expert Rev. Proteomics* **2014**, *11*, 649–651.
[11] T. K. Toby, L. Fornelli, N. L. Kelleher, *Annu. Rev. Anal. Chem.* **2016**, *9*, 499.
[12] A. Lesur, B. Domon, *Proteomics* **2015**, *15*, 880–890.
[13] A. J. Hughes, D. P. Spelke, Z. Xu, C.-C. Kang, D. V. Schaffer, A. E. Herr, *Nat. Methods* **2014**, *11*, 749–755.
[14] J. C. Tran, L. Zamdborg, D. R. Ahlf, J. E. Lee, A. D. Catherman, K. R. Durbin, J. D. Tipton, A. Vellaichamy, J. F. Kellie, M. Li, C. Wu, S. M. M. Sweet, B. P. Early, N. Siuti, R. D. LeDuc, P. D. Compton, P. M. Thomas, N. L. Kelleher, *Nature* **2011**, *480*, 254–258.
[15] R. A. O'Neill, A. Bhamidipati, X. Bi, D. Deb-Basu, L. Cahill, J. Ferrante, E. Gentalen, M. Glazer, J. Gossett, K. Hacker, *Proc. Natl. Acad. Sci. USA* **2006**, *103*, 16153–16158.
[16] P. G. Righetti, *Isoelectric Focusing: Theory, Methodology and Application*, Elsevier, Amsterdam, **1983**.
[17] A. J. Hughes, A. M. Tentori, A. E. Herr, *J. Am. Chem. Soc.* **2012**, *134*, 17582–17591.
[18] J. J. Li, P. J. Bickel, M. D. Biggin, *PeerJ* **2014**, *2*, e270.
[19] B. Schwanhäusser, D. Busse, N. Li, G. Dittmar, J. Schuchhardt, J. Wolf, W. Chen, M. Selbach, *Nature* **2011**, *473*, 337–342.

[20] A. M. Tentori, A. J. Hughes, A. E. Herr, *Anal. Chem.* **2013**, *85*, 4538 – 4545.
[21] C.-C. Kang, J.-M. G. Lin, Z. Xu, S. Kumar, A. E. Herr, *Anal. Chem.* **2014**, *86*, 10429 – 10436.
[22] A. J. Hughes, R. K. Lin, D. M. Peehl, A. E. Herr, *Proc. Natl. Acad. Sci. USA* **2012**, *109*, 5972 – 5977.
[23] B. Bodenmiller, E. R. Zunder, R. Finck, T. J. Chen, E. S. Savig, R. V. Bruggner, E. F. Simonds, S. C. Bendall, K. Sachs, P. O. Krutzik, G. P. Nolan, *Nat. Biotechnol.* **2012**, *30*, 858 – 867.
[24] C. G. Horvath, S. R. Lipsky, *Anal. Chem.* **1967**, *39*, 1893.
[25] T. A. Duncombe, C. C. Kang, S. Maity, T. M. Ward, M. D. Pegram, N. Murthy, A. E. Herr, *Adv. Mater.* **2016**, *28*, 327 – 334.
[26] C.-C. Kang, K. A. Yamauchi, J. Vlassakis, E. Sinkala, T. A. Duncombe, A. E. Herr, *Nat. Protoc.* **2016**, *11*, 1508 – 1530.
[27] P. Verdier-Pinard, F. Wang, L. Martello, B. Burd, G. A. Orr, S. B. Horwitz, *Biochemistry* **2003**, *42*, 5349 – 5357.
[28] J. V. Forment, S. P. Jackson, *Nat. Protoc.* **2015**, *10*, 1297 – 1307.
[29] S. Lebel, C. Lampron, A. Royal, Y. Raymond, *J. Cell Biol.* **1987**, *105*, 1099 – 1104.
[30] J. Nilsson, M. Evander, B. Hammarström, T. Laurell, *Anal. Chim. Acta* **2009**, *649*, 141 – 157.
[31] C. Vogel, E. M. Marcotte, *Nat. Rev. Genet.* **2012**, *13*, 227 – 232.
[32] Z. R. Gregorich, Y. Ge, *Proteomics* **2014**, *14*, 1195 – 1210.

Received: June 21, 2016
Published online: September 6, 2016

